[1]Vinodini Bhole

[2] Dr.Sanjay Dambhare

Augmented SPWM based Hybrid Output Converter for Renewable Energy and Nano-Grid Application

Journal of Electrical Systems

Abstract: - This study suggests a novel Augmented Sine PWM(ASPWM) based Hybrid Output Converter that can concurrently power AC and DC loads. Two boost converters are used in this configuration, and the AC voltage is the differential voltage tapped between the two source nodes (of the MOSFETs) of the individual converters. This converter plays a different role in providing power to AC and DC loads than conventional boost converter. Conventional boost requires a minimum of two stages to step up output DC voltage and inverter stage to convert DC to AC power. This novel hybrid output converter (HOC) skips all stages of boosting the output voltage and next stage of inverter also. HOC consists of two boost converts pumped by two VM(voltage multiplier) stages to get high voltage DC output. This HOC has two inputs, supplied by renewable like solar PV cells and has two outputs to supply AC and DC loads simultaneously. This dual input HOC integrates two renewable inputs for standalone nano grid application. The principle of operation of HOC is augmented sinusoidal pulse width modulation with AC reference signal is shifted by $180^0$for individual boost converter and augmented by dc offset. The circuit has been extensively simulated in PSIM'22 Matlab Simulink and an experimental prototype of 110W is tested in the laboratory.

Keywords: Augmented Space Vector Modulation (Aspwm), Hybrid output converter (HOC),Nano grid, Renewable,Two input two output.

I. INTRODUCTION

DC-DC converters are bridges between integration of renewable energy sources and electrical grid or other AC and DC demands. When the grid requirement is of high DC and AC voltage simultaneously, conventional (SISO) boost converters are configured every time, when combined with inverters. Currently the only option left is renewable energy because fossil fuels are running out, energy demand is growing, and CO2 emissions are causing air pollution. In [1],It is discovered that using renewable energy to supply power electronics circuits and variable speed drives necessitates repeated DC-DC and DC-AC conversions, which reduces overall system efficiency. The optimum DC voltage level for the DC micro grid is identified from relevant case studies, and it is suggested that the DC system will have a 22 % total efficiency gain over the traditional AC grid system. Compared to modular conversion stages, single-stage conversion systems use fewer components, which leads to easier control mechanisms and higher efficiency. To obtain the AC and DC outputs at the same time from different DC sources, complex parallel-operated conversion stages are required. When it comes to integrating these sources, multi-port converters come out on top because they are effective power interfaces that link renewable energy sources to the grid. In[2], a control technique for power balancing between input sources and output voltages is developed, and a multi input multi output(MIMO) topology for boost converters in which a single inductor connects several inputs and loads simultaneously is proposed. In[3],a proposed MIMO DC-DC boost converter that describes energy source hybridization and is designed for deployment in electric vehicles. There are two modes of operation for the converter: charging and draining of the battery. There are two inputs, two outputs, and a single inductor in the proposed MIMO converter. In [4], a high gain converter is proposed where fuel cell, photo voltaic panel and battery are the three inputs and one dc output. Fuel cell is considered as main input and rooftop PV solar cell is the other one, charges battery when required. In [5],basic configuration of four input two outputs is described (MIMO converter). This MIMO DC-DC boost converter has four inputs and two outputs. The two inputs out of four are decoupled with two DC outputs while two inputs are coupled. This structure provides integration of renewable inputs with DC batteries so that high gain DC obtained at the output. The diode-capacitors (VM) voltage multiplier stages are responsible for enhancing DC output voltage. In[6] for moderate DC voltage microgrid applications, a multi-port bipolar DC-DC isolated converter is suggested, with three ports designated specifically for fuel cell, solar, and battery inputs. The bipolar DC micro grid is supplied by two series coupled DC outputs. The circuit is bulky and complex due to the utilization of twelve switches and a high-frequency transformer. [7] With integrated inputs for solar PV panels, wind turbines, and rechargeable batteries used for hybrid energy applications, it offers

[1] *Corresponding author: Author 1 Affiliation

[2] Author 2 Affiliation

an isolated DC-DC converter for a stand-alone system. Various types of controllers are designed to control the DC link voltage, battery voltage and current. In[8],a new four-port DC-DC converter is proposed for low-voltage bipolar DC micro grid to interface renewable sources. Due to one inductor and few switches, it has low switching losses. The converter is configured with two output capacitors connected in series. A non-isolated symmetric four-port (DIDO)converter is presented in [9]. This converter is bipolar and connects PV, battery system, and low voltage DC micro grid. According to the application, it works on several modes like SISO, DIDO, and SIDO. The proposed converter is said to be several MPCs for DC micro grids. To connect solar PV cells and for battery charge discharge, three switches are configured and hence this is a multi-port converter. Its output voltage is bipolar. In[10], five port DC-DC converter is presented. It consists of three solar-pv input ports, battery storage and two high gain DC outputs. It consists of twelve switches to rectify and invert AC to DC supply up to 380V to DC micro grid. In [11] multi-port converter is configured to provide AC voltage with less harmonic distortion and moderate bipolar DC voltage. One of the ports of the converter is connected to a multilevel inverter to provide AC voltage. In [12], several multiport converter configurations are studied like SIMO, MISO, and MIMO converters to connect renewable sources and DC microgrids.

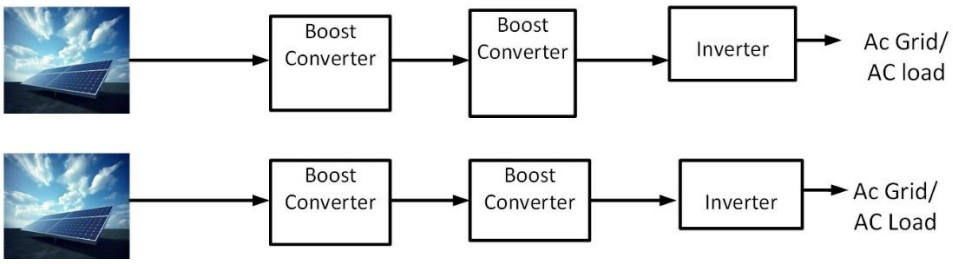

Fig1(a): Conventional Converter and AC grid

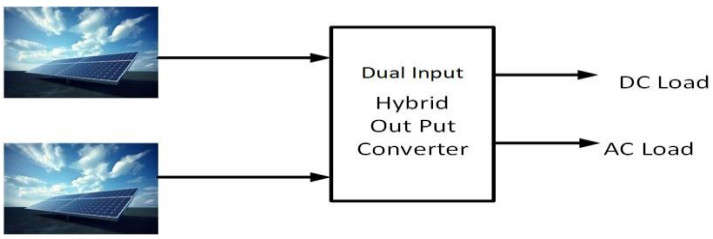

Fig1(b): Hybrid Output Converter

Due to simultaneous demand of AC and DC power, hybrid converters are now part of hybrid micro grid system. Conventionally, DC power is fed to dc load directly as the output of a high gain DC-DC converter due to demand of high voltage DC. The inverter in the circuit provides AC power if required.Fig.1 explains the role of hybrid output converter in DC Micro grid in comparison with conventional converter inverter system. In[13],AC DC (SIMO)boost converter where one power switch is replaced by full bridge inverter is presented. It is an interleaved hybrid converter where input current is divided by interleaved inductor. Hybrid converter functions in three modes, power mood shoot through mode and intermediate mode. In[14], the hybrid converter designed with one input but input currents is splitted into two circuits. One circuit is a bridge inverter, and the other is boosting converter. The switch in the boost converter is replaced by a full bride inverter. Switching strategy is modified to get simultaneous AC and DC power. In[15],hybrid converter with interleaved inductor and one power switch supplies AC and DC loads using ASPWM technique is presented. In[16],The topology proposed in this paper is a hybrid converter configured with of two inputs and two hybrid (Ac and DC) outputs.

The topology proposed in this paper is a hybrid output converter configured with two inputs and two hybrid (Ac and DC) outputs. This topology, which is outcome of two boost converters and two diode capacitors (VM) stages, produces stepped-up DC voltage. An ASPWM technique is implemented in this converter to produce AC and DC output at the same time. In remote or rural areas, to produce and utilize AC and DC power in one stage, hybrid converter is proposed. It is applicable to rooftop nano grid applications. It is a perfect option to supply a system with a small capacity AC voltage and a moderate DC voltage where solar energy is available abundantly.

The paper is organized as follows: Section II describes the proposed hybrid output converter, explanation of

modes of the operation and the concept of ASPWM switching briefly. Section III contributes the design of passive components. Section IV, study of state space modeling of the hybrid converter is presented. Section V depicts simulation results. In section VI, a light is thrown upon hardware results and comparison. Section VII elaborates analysis of converter efficiency and section VIII concludes the paper.

II. PROPOSED HYBRID OUTPUT CONVERTER CONFIGURATION AND OPERATING PRINCIPLES

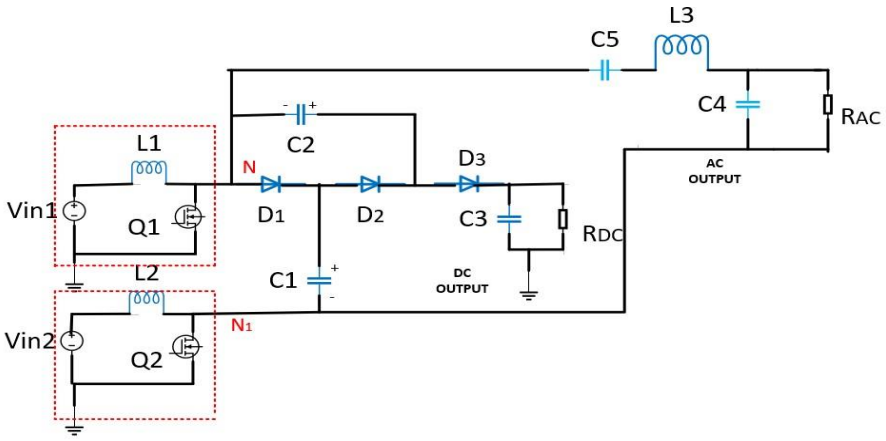

Fig 2: Hybrid Output Converter

The proposed hybrid output converter is introduced in Fig.2, where two boost converters are highlighted with red dotted lines. Q_1 and Q_2 are the switches $L_1$and $L_2$are the two inductors of the two boost converters. Inductor L_3 and capacitor C_5 are the components of LC filter. Capacitor C_3filters DC output. V_{in1} and V_{in2} are the input voltage sources (obtained from solar PV cells and or battery) and across load Rdc and Rac outputs Vdc and Vac are obtained. The DC voltage in the hybrid output converter is acquired by combining outputs of two boost stages and AC output is collected by filtering the resultant nodal voltage obtained at two nodes of boost stages. The two nodes are termed as N and N_1 The proposed hybrid converter provides a high gain DC output and an AC voltage with negligible harmonic distortion. D_1, D_2 and C_1 and C_2 are diodes and capacitors of voltage multiplier stages.

To develop switching signals, two sinusoidal modulating signals with phase difference of 180^0 and of power frequency are added with DC offset(d) and they are compared with triangular carrier signal of 10kHz. ASPWM signals are generated at nodes of each boost stage carrying 10kHz frequency each. The resulting voltage derived across inductors L_1 and L_2 carries 50Hz component which is 180^0out of phase. The corresponding difference in two nodal voltage across the nodes at two boost stages as shown in Fig.2,is filtered to get 50Hz AC output. The filter capacitance of DC output is adequate to get ripple free constant voltage throughout the function. The operation of the hybrid output converter and ASPWM technique are discussed in detail in the next sessions.

A. Function of proposed Hybrid Output Converter

The hybrid output converter (HOC) operates in four modes. The modes are different in sequence during positive and negative half cycles of modulating wave, The HOC operates in three modes out of four in each half cycle. The operation of converter and operating modes in positive and negative cycles are explained in the subsections eventually. One cycle of the modulating wave is selected and all modes of operations in positive and negative half cycle of modulating waveform of the circuit are explained.

B. Operating Modes

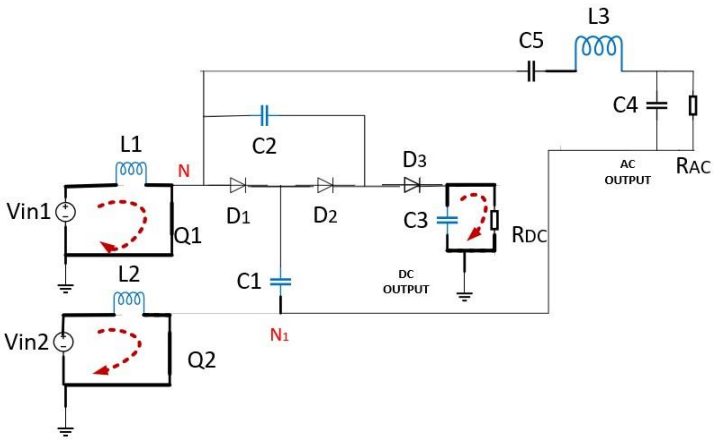

Fig 3(a): Mode 1, When Q_1 and Q_2 both switches are ON

Mode 1: Both switches Q_1 and Q_2 are ON. (This mode appears in both positive and negative half cycles) From equivalent circuit in fig.3 (a), the mode I is illustrated as follows. When Q_1 and Q_2 both are ON, Inductor current 1_{L1} and I_{L2} flow and inductors L_1 and L_2 are energized. Capacitor C_3 discharges through the load. In this mode the following equations are obtained.

$$\frac{diL2}{dt} = \frac{Vin2}{L2} \quad (1)$$

$$\frac{diL1}{dt} = \frac{Vin1}{L1} \quad (2)$$

$$\frac{dVC1}{dt} = 0 \quad (3)$$

$$\frac{dVC2}{dt} = 0 \quad (4)$$

$$\frac{dVC3}{dt} = -\frac{VC3}{Rdc*C3} \quad (5)$$

Mode 2 : First Switch will be ON and second switch will be OFF. (Q_1 ON and Q_2 OFF) This mode appears in positive half cycle only. From equivalent circuit in fig.3 (b), mode 2 is elaborated as follows. When Q_1 ON and Q_2 OFF, Inductor current I_{L2}flows to charge the capacitor $C_1$and C_2 and forward biases diode D_2. D_1 and D_3 are reverse biased. Capacitor C_3 discharges through load Rd. The relevant equations for the second mode are as follows,

$$\frac{diL1}{dt} = \frac{Vin1}{L1} \quad (6)$$

$$\frac{diL2}{dt} = \frac{Vin2+VC1-VC2}{L2} \quad (7)$$

$$\frac{dVC1}{dt} = \frac{Il2}{C1} \quad (8)$$

$$\frac{dVC2}{dt} = \frac{Il2}{C2} \quad (9)$$

$$\frac{dVC3}{dt} = -\frac{VC3}{Rdc*C3} \quad (10)$$

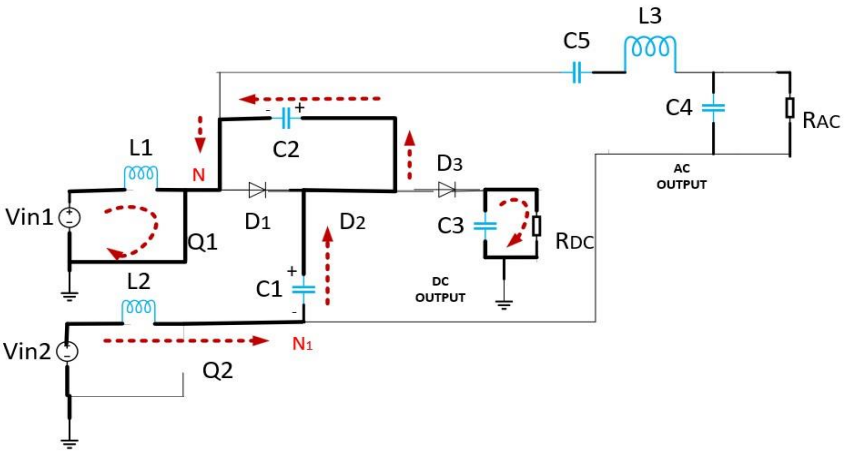

Fig 3(b): Mode 2, When Q_1 is ON and Q_2 is OFF

Mode 3: $Q_1$is OFF and Q_2 is ON) (This mode appears in negative half cycle only.) From equivalent circuit in fig.3 (c), mode 3 is explained as follows. When $Q_1$is OFF and Q_2 is ON, Inductor current I_{L1} flows to charge the capacitor C_1 and forward biases diode D_1. D_2 and $D_3$are reverse biased. The relevant equations for the third mode are as follows.

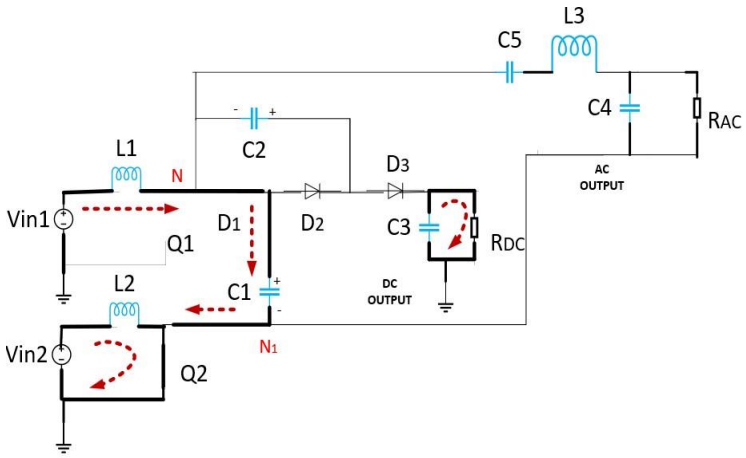

Fig 3(c): Mode 3, When Q_2 is ON and Q_1 is OFF

$$\frac{diL2}{dt} = \frac{Vin2}{L2} \quad (11)$$

$$\frac{diL1}{dt} = \frac{Vin1-VC1}{L1} \quad (12)$$

$$\frac{dVC2}{dt} = 0 \quad (13)$$

$$\frac{dVC1}{dt} = \frac{Il1}{C1} \quad (14)$$

$$\frac{dVC3}{dt} = -\frac{VC3}{Rdc*C3} \quad (15)$$

Mode 4 : When both switches Q_1 and Q_2 are OFF. From equivalent circuit in fig.3(d), mode 4 is described as follows. When Q_1 and Q_2 are OFF, Inductor current I_{L1} flows to charge the capacitorC_2 forward biases diodeD_3 and supplies load. Simultaneously Inductor current I_{L2} flows to charge the capacitor C_1, forward biases diode D_2 and supplies load. The relevant equations for the fourth mode are as follows.

$$\frac{diL2}{dt} = \frac{Vin2+VC1-VC3}{L2} \quad (16)$$

$$\frac{diL1}{dt} = \frac{Vin1+VC2-VC3}{L1} \quad (17)$$

$$\frac{dVC2}{dt} = \frac{Il1}{C2} \quad (18)$$

$$\frac{dVC1}{dt} = \frac{Il2}{C1} \quad (19)$$

$$\frac{dVC3}{dt} = \frac{Il1}{C3} + \frac{Il2}{C3} - \frac{VC3}{Rdc*C3} \quad (20)$$

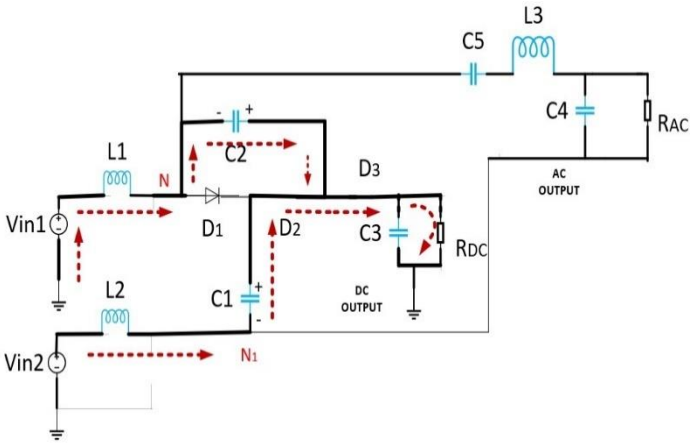

Fig 3(d): Mode 4, When Q_2 and Q_1 both are OFF.

For a one cycle of 20 ms period average AC voltage is zero at the ac filter circuit, so the ac voltage is not considered in deriving the voltage equation of proposed converter. Due to ASPWM technique, it is observed that during positive half cycle converter undergo mode1.mode 2 and mode4 operations. And during negative half cycle converter undergo mode 1, mode 3, mode 4 operations which is depicted in fig.4.

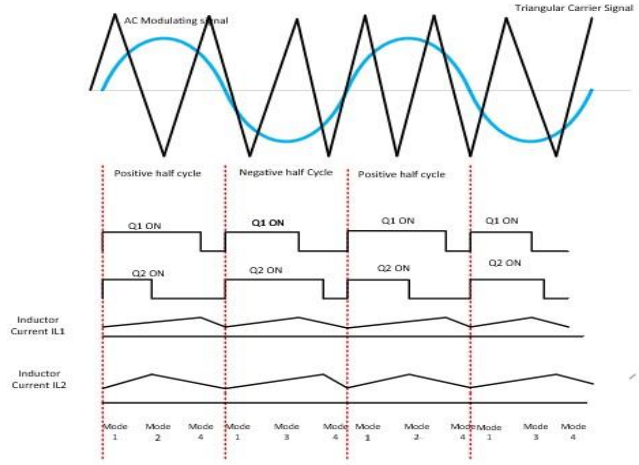

Fig.4: Operating Modes in both half cycles of modulating AC signal

In a steady State condition, the average voltage across the inductor should be zero due to volts-second balance law. Applying volts second balance law for the inductor voltages of $L_1$and L_2, in Positive half cycle,
The output voltage across capacitor C3 termed as VC3 is obtained by:

$$\text{Vout}= \frac{1}{2}\left[\frac{Vin1}{(1-D1)}+\frac{Vin2}{(1-D2)}+VC1+VC2\left(\frac{1-D2}{1-D1}\right)\right] \quad (21)$$

In negative half cycle,

$$\text{Vout}= \frac{1}{2}\left[\frac{Vin1}{(1-D1)}+\frac{Vin2}{(1-D2)}+VC1\left(\frac{1-D2}{1-D1}\right)+VC2\right] \quad (22)$$

C ASPWM Principle

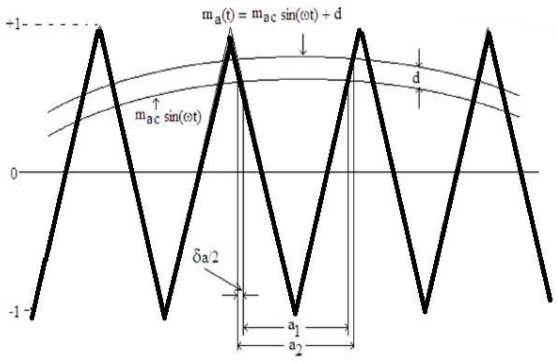

Fig.5: ASPWM Principle

The ASPWM principle for the generation of AC voltage in the proposed hybrid output converter is explained in detail in the reference paper. [16] The effective value of duty cycle D is augmented by d in the modulating signal, averaging over 20 ms is given by equation (24).

$$D=0.5(d+1) \quad (23)$$

For duty ratios D_1 and D_2

$$D1=0.5(d_1+1) \quad (24)$$
$$D2=0.5(d_2+2) \quad (25)$$

Output Voltage: $Vo_{utput} = \frac{Vin1}{(1-d1)} + \frac{Vin2}{(1-d2)} + \frac{1}{2}(VC1 + VC2)$ (26)

It can be concluded from equation (26) that DC offset value d controls DC output voltage.
AC output voltage can be calculated as follows.

$$V_{ac} = m_{ac} \times V_{dc} \times 0.8 \quad (27)$$

where 0.8 is a attenuation factor due to filter circuit.

III. DESIGN OF PASSIVE COMPONENTS

A. Design of Inductor

Considering CCM operation inductor value is designed. Current ripple is allowed up to 35% L1 and L2 are computed as follows:

$$\Delta I_{L1} = \frac{D_{1max} \times V_{in1}}{F_s \times L_1} \quad (28)$$

$$\Delta I_{L2} = \frac{D_{2max} \times V_{in2}}{F_s \times L_2} \quad (29)$$

Where $D_1$and $D_2$are duty ratios of switches Q_1 and Q_2 Fs is the switching frequency and V_{in1} and V_{in2} are input voltages.

$$L_{1min} \geq \frac{D_{1max} \times V_{in1}}{F_s \times \Delta I_{L1}} \ , L_{2min} \geq \frac{D_{2max} \times V_{in2}}{F_s \times \Delta I_{L2}} \quad (30)$$

B. Design of Capacitor

Capacitor values are designed considering \$5\$ \% voltage ripples at the output.

$$C_{out} = \frac{D \times I_{avgD}}{F_s \times \Delta V_c} \quad (31)$$

$$C_{VMstage} = \frac{I_{avgD}}{F_s \times \Delta V_c} \quad (32)$$

The values of inductor L_1 and L_2 and VM capacitors C_1, C_2 C_3 at output) are calculated from the above equations. The obtained values of the passive components are L_1=4.7 mH and L_2=4.7 mH, C_1=C_2=470µF and C_3 at output=2. 2mF.Additionally, it is possible to calculate the values of the two ac filter components L_F and C_F by keeping gain unity, at 50 Hz (line frequency) and 40 dB attenuation for the high frequency component.

C. Design of Diodes

In the proposed HOC diodes are used as part of VM stages. Two VM stages are configured in this hybrid converter. Voltages across capacitors in VM stages decide the limit of voltage stress on diode. DC output voltage is always greater than voltage stress across diode.

$$V_{Distress} = \frac{1}{(1-D)} V_{in1} \quad (33)$$

According to modes of operation, average current of all diodes in VM stages during one period of switching is given as

$$I_{D1\,2\,3} = I_{outDC} \quad (34)$$

D. Design of Power Switches

In the proposed hybrid converter two switches are shunted across voltages sources due to boosting action. When they are on OFF condition, they must withstand maximum voltage developed across converter. The general equation of voltage stress across power switch for the converter is as follows.

When the switches are in ON condition the whole input current flows through the switch.

$$V_{Sistress} = \frac{1}{(1-D)} V_{in1} \quad (35)$$

$$I_{Siavg} = \frac{1}{(1-D)} I_{outDC} \quad (36)$$

IV. STATE SPACE ANALYSIS

From the operating voltage and current equations derived in section II, all inductor voltages and capacitor voltages are considered as state variables and in the steady state input voltages are control variables.

During positive half Cycle, Mode 1, Mode 3 and Mode 4 are active.

$$X = A\dot{X} + BU$$
$$Y = CX + DU \quad (37)$$

$$X = [\dot{I_{L1}} \quad \dot{I_{L2}} \quad \dot{V_{c1}} \quad \dot{V_{c2}} \quad \dot{V_{c3}}]^T \quad (38)$$

$$B = \begin{bmatrix} \frac{1}{L_1} & 0 & 0 & 0 & 0 \\ 0 & \frac{1}{L_2} & 0 & 0 & 0 \end{bmatrix}^T$$

$$U = [V_{in1} \quad V_{in2}]^T \quad (39)$$

$$C = [0 \quad 0 \quad 0 \quad 0 \quad 1] \quad (40)$$

Mode 1

$$A_1 = \begin{bmatrix} 0 & 0 & 0 & 0 & 0 \\ 0 & 0 & 0 & 0 & 0 \\ 0 & 0 & 0 & 0 & 0 \\ 0 & 0 & 0 & 0 & 0 \\ 0 & 0 & 0 & 0 & -\frac{1}{Rdc*C3} \end{bmatrix} \quad (41)$$

Mode 3

$$A_3 = \begin{bmatrix} 0 & 0 & 0 & 0 & 0 \\ 0 & 0 & \frac{1}{L_2} & \frac{-1}{L_2} & 0 \\ 0 & \frac{1}{C_1} & 0 & 0 & 0 \\ 0 & \frac{1}{C_2} & 0 & 0 & 0 \\ 0 & 0 & 0 & 0 & -\frac{1}{Rdc*C3} \end{bmatrix} \quad (42)$$

Mode 4

$$A_4 = \begin{bmatrix} 0 & 0 & 0 & 0 & 0 \\ 0 & 0 & \frac{1}{L_2} & \frac{-1}{L_2} & 0 \\ 0 & \frac{1}{C_1} & 0 & 0 & 0 \\ 0 & \frac{1}{C_2} & 0 & 0 & 0 \\ 0 & 0 & 0 & 0 & -\frac{1}{Rdc*C3} \end{bmatrix} \quad (43)$$

$$A = A_1 + A_3 + A_4 \quad (44)$$

Similarly, for negative half cycle mode1, mode2, mode4 are active. Mode 1 and mode 4 are common in both cycles.

Mode 2

$$A_2 = \begin{bmatrix} 0 & 0 & \frac{1}{L_1} & 0 & 0 \\ 0 & 0 & 0 & 0 & 0 \\ \frac{1}{C_1} & 0 & 0 & 0 & 0 \\ 0 & 0 & 0 & 0 & 0 \\ 0 & 0 & 0 & 0 & -\frac{1}{Rdc*C3} \end{bmatrix} \quad (45)$$

$$A = A_1 + A_2 + A_4 \quad (46)$$

the controllability matrix of this system is defined as follows:

$$Q_c = [A \quad AB \quad A^2B \quad - \quad A^{n-1}B] \quad (47)$$

Where n is its rank. QC=5which is rank of A matrix so it is completely controllable.

V. SIMULATION RESULTS

The proposed hybrid output converter has been simulated in MATLAB. The performance of the proposed converter is justified through simulation results. This converter is presented and studied as a new topology in hybrid converter family. It has two inputs and two hybrid outputs. Inputs can be renewable devices and or storage devices to obtain high gain DC and low distorted AC. Proposed hybrid converter is simulated into two input voltage ranges,30 V,48 V and 8 V,15 V. Due to ASPWM switching variable width PWM signal generation is possible.

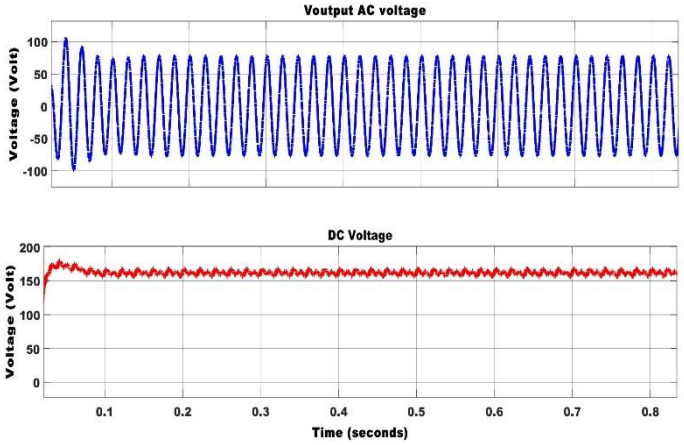

Fig.6: Simulation Results of Proposed hybrid Converter at Input Voltages 30V and 48 V

When V_{in1} is 30V and V_{in2} is 48V, DC output voltage obtained is 160V and AC RMS voltage is 55V under CCM operation of inductor currents as shown in Fig.6.

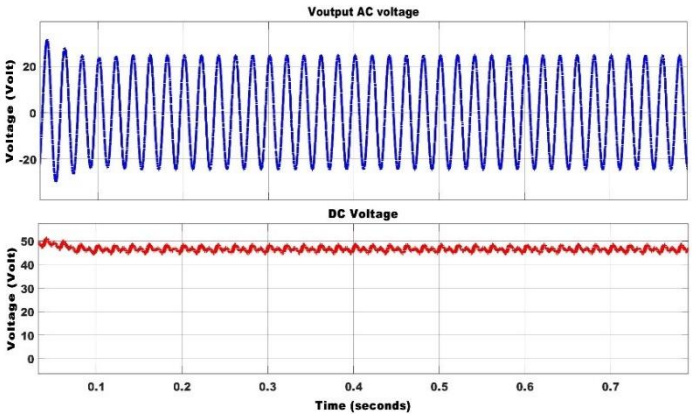

Fig.7: Simulation Results of Proposed hybrid Converter at Input Voltages 8V and 15 V

When V_{in1} is 8V and V_{in2} is 15V, DC output voltage obtained is 46V and AC RMS voltage is 22V under CCM operation of inductor currents as shown in Fig.7.

	BDHC [14]	IHC [13]	BBDHC [15]	Proposed HOC
Input Voltage	48V	48V	12V	30V and 48V
OutPut DC	100 V DC	194 VDC	15V DC	160V DC
Output AC	30 V RMS	38V RMS	5 V RMS	55 V RMS

Table I: Comparison between existing hybrid converters based on DC Microgrid application.

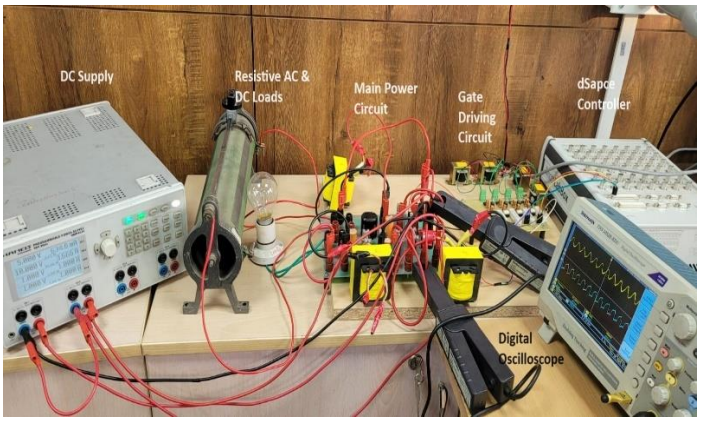

Fig.8: Hardware of Proposed Hybrid Output Converter Circuit

VI EXPERIMENTAL RESULTS

The power and control circuit of hybrid output converter has been tested at steady state on 100 W laboratory prototype at various input voltages. DC and AC output voltages are verified experimentally, analytically and by simulation to prove the topology of hybrid converter. During the experimentation the condition of $d+M \leq 1$ is maintained to avoid over modulation by selecting d as a 0.2 and M as a 0.7 throughout the operation. Passive components are selected to maintain continuous operating mode. Dspace micro lab setup and gate driving circuit are the parts of switching circuit. Dspace micro lab controller is used to generate switching gate pulses. These pulses are conveyed to the driver circuit for isolation and amplification. These isolated and amplified pulses drive switches Q_1 and Q_2 in the power circuit of hybrid output converter.

	Conventional	BDHC [14]	IHC [13]	BBDHC [15]	Proposed HOC
Switch Count	7	4	5	2	2
Switching Technique	SPWM	Modified unipolar SPWM	Modified unipolar SPWM	ASPWM	ASPWM
Type of Inputs and count		Renewable or Battery,1	Renewable or Battery,1	Renewable or Battery,1	Renewable and/or Battery,1
Shoot through Protection	No	yes	yes	yes	yes

Control parameters	No Condition	$D + M \leq 1$	Independent	$d + M \leq 1$	$d + M \leq 1$
Maximum Efficiency	82%	86%	91%	91.6%	91.8%

Table II: Comparison between conventional converter, hybrid converter and proposed hybrid output converter

Description	Parameter	Value	Unit
Inductors	L_1 L_2	4.7	mH
Capacitors	C_1 C_2	470	µF
DC output Capacitor	C_3	2.2	mF
AC output Capacitor	C_5	470	µF
Load (AC and AC)	20Ω,20Ω		
filter circuit Inductor	L_3	50	mH
filter circuit Capacitor	C_4	440	µF
Switching Frequency	SwFr	10	kHz

Table III: Parameters of proposed hybrid converter

The proposed hybrid output converter is configured with two boost cells cascaded in a fashion to deliver high gain DC voltage and distortion free AC. Table I shows comparison between existing hybrid converters in the literature and proposed hybrid output converter for DC micro grid application. Table II represents comparison between existing hybrid converters in the literature and proposed hybrid output converter based on number of components and configuration, switching technique and efficiency. List of passive components used in proposed converter is given in the Table III and Table IV indicates other components and controllers used to generate pulses along with their details. The laboratory experimental set up of proposed hybrid output converter is shown in Fig.8.

Component	Commercial Name
MOSFET	IRF250N
Diodes	FEP30JP
Optocoupler	TLP350
Voltage Regulator	L7815CV
Controller	dSpace Microlab Box

Table IV: Components used in Proposed Hybrid Output Converter

In table V comparison of the results by hardware, simulation and analytical is presented at equal input and load condition.

	Hardware Result	Simulation Result	Analytical Result
AC Output Voltage	19.4 V RMS	21V RMS	28V RMS
DC Output Voltage	39.6V	46V	42V

A. Steady State Results

In this section steady state outputs of proposed hybrid converter are presented. The switching signals are shown in Fig.9(a), (b),(c).These three switching waveforms are captured at random three instants. It is observed that pulse widths are sinusoidally varying in nature and enhanced due to DC offset d as explained in the earlier section. The switching pulses are given to switches Q_1 and Q_2. Resulting nodal voltage at nodes N and $N_1$is obtained in AC form by action of LC filter at fundamental frequency of 50 Hz.Fig.10,11 and Fig.12 show inductor currents, DC output voltage and AC output voltages at input voltage 8 V and 15 V. Both AC and DC loads are resistive in nature.

Table I indicates comparison of the simulated and hardware outputs of proposed hybrid converter prototype. The maximum observed efficiency based on it was around 91.8\% for the above experimental conditions. Following points are to be noted about Hybrid Output Converter

- All devices configured in the proposed hybrid converter are considered as ideal.
- Hybrid converter studied and presented as a new topology to cater number of renewable sources during daytime to charge batteries and simultaneously supply any small AC load.

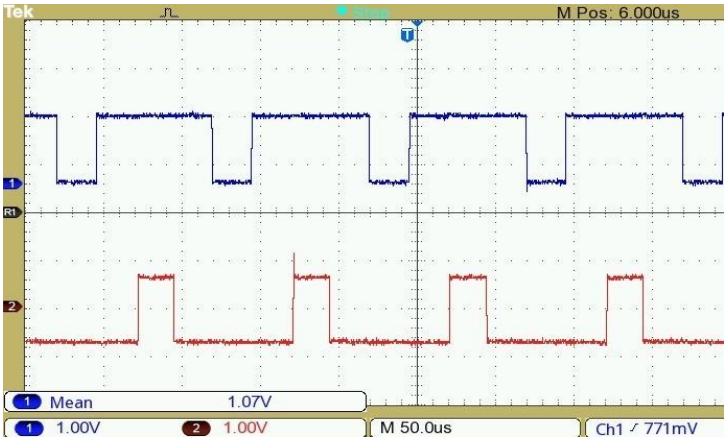

Fig.9: (a)PWM1

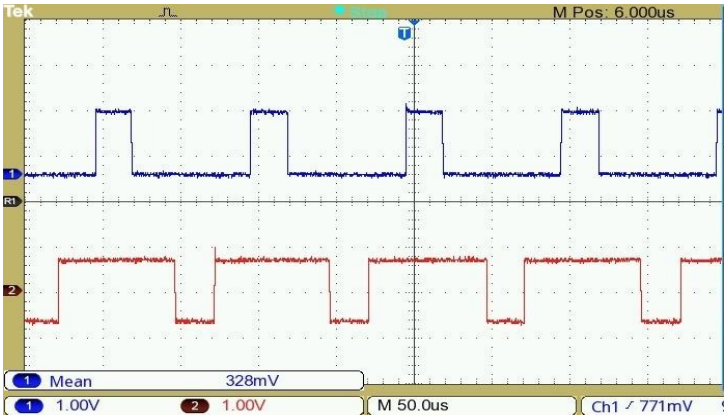

Fig.9: (b)PWM2

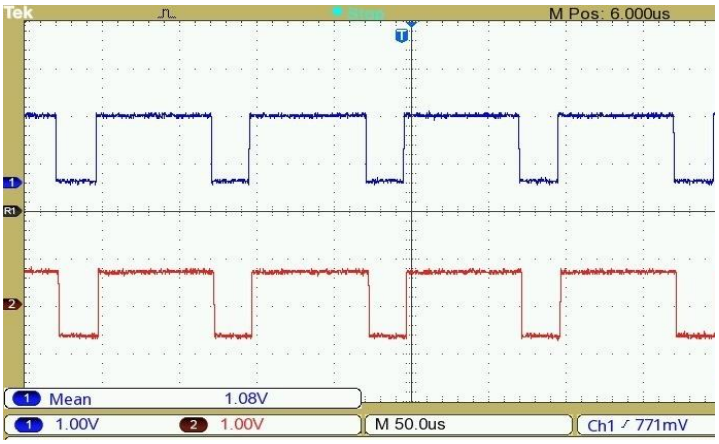

Fig.9: (c)PWM3

Inductor Currents are in continuous conduction mode. Inductor currents are 1.67A and 6.26A respectively.

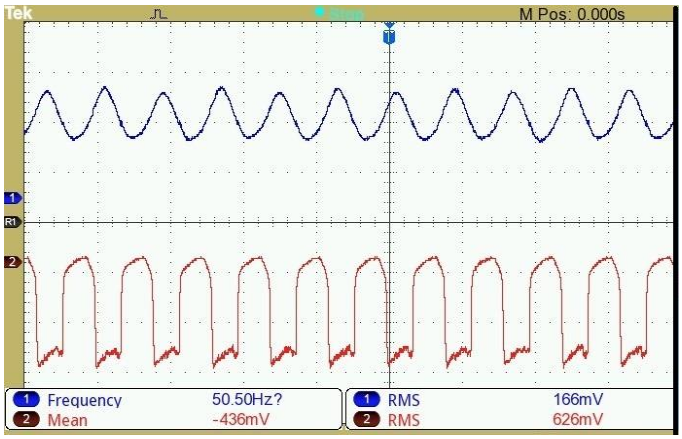

Fig.10: Inductor Currents at input voltages 8V and 15 V

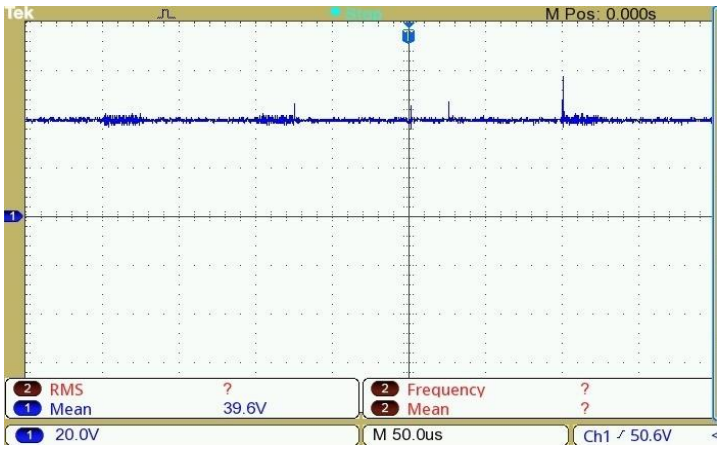

Fig.11: DC output voltage at input voltages 8V and 15 V

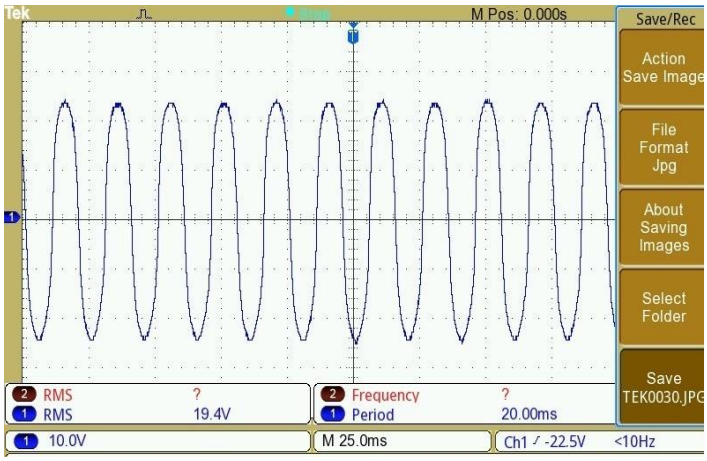

Fig.12: AC output voltage at input voltages 8V and 15 V

B. Comparison

Table I indicates comparison of the simulated and hardware outputs of proposed hybrid converter prototype. The maximum observed efficiency based on it was around 91.8\% for the above experimental conditions.

In the table II, comparison between proposed hybrid output converter and conventional converter inverter set and other hybrid converters configurations in the literature is presented. Conventional converters can integrate one renewable source at a time. It requires an inverter to supply AC load. With addition of inverter the number of switches and gate driving circuitry increases switching losses hence it affects overall efficiency of the system.

Conventionally it reaches 85\% For all together AC and DC outputs, all hybrid converters have two boost converters configured into a single device. Boost Derived Hybrid Converters (BDHC) [14] and Interleaved Hybrid Converters (IHC) [13] are presented in the literature using a novel circuit ideas and new control methods. The (BDHC) uses an H-bridge instead of one switch in conventional boost converter and inverter circuit. This brings down the number of switches to four and claims inherent shoot through protection. (IHC), has two distinct currents paths for AC and DC outputs due to interleaved inductor. One switch is replaced by full bridge inverter circuit in one of the two boost converters. The proposed Hybrid output Converter has the following features which are comparable with the other IHC [13],BDHC[14]and BBIHC[15]hybrid converters.

- Hybrid output converter has two inputs to cater two renewable inputs simultaneously or one of the inputs can be battery if required.
- Three inductors and two switches make the configuration simple and less bulky.
- The proposed hybrid output converter can provide high gain DC and low THD AC voltage which is more than other hybrid converters with low switching losses.

VII EFFICIENCY ANALYSIS

A Losses in Power Switches

The switching losses in Q_1 and Q_2. The switching loss per cycle is given by.

$$P_{Q1sw} = \frac{1}{T}\left[\int_0^{ton} V_{in1}\left(1-\frac{t}{ton}\right)\left(I_1\frac{t}{ton}\right)\right]dt + \frac{1}{T}\left[\int_0^{toff}\left(V_{in1}\frac{t}{toff}\right)\left(I_1-\frac{I_1 t}{toff}\right)\right]dt \quad (48)$$

From equation (48) switching loss of $Q_1$is calculated. Similarly Switching loss of Q_2 is calculated. Where I_1 is the current through Q_1.T_{off} =55 nS and T_{ON}=17nS for IRFP250N switches.

Conduction Losses the switches are calculates as follows:
$(I \times D)^2 R_{dsON}$ where D is a duty ratio and R_{dsON} is ON state resistance of the switch. Now d is dc offset and $D = 0.5(1+d)$.

$$Total\ Conduction\ loss = {I_1}^2(0.5(1+d))^2 \times 0.075 + {I_2}^2(0.5(1+d))^2 \times 0.075 \quad (49)$$

Substituting I_1=1.6A and I_2= 6.26 A and R_{dsON}=0.075Ω,
Total Conduction Loss=1.058W and Switching loss is negligible.

B Losses in Diode

Diode switching loss is given by:

$$P_{Dsw} = \frac{1}{T}\left[\int_0^{ta}\left(\frac{I_{RM}}{T_{off}}V_D\right)dt\right] + \left[\int_0^{tb}\left(\frac{I_{RM}}{T_b}V_{Dcout}\right)dt\right] \quad (50)$$

Where I_{RM}=10μA, V_D =1.5V, $V_{Dcout} = 50V$,$T_{OFF} = 7 \times 10^{-5} Sec$
$T_a = T_a = \frac{T_{rr}}{2}$,$T_{rr} = 50nS$ for diode FEP3JP. Switching loss is negligible.
$Conduction\ Loss = 3 \times V_D \times I_D \times D$, $I_D = 1.35A$,D=0.6
$Conduction\ Loss = 3.456W$

C Losses in Reactive Elements

ESR of L_1 and L_2=0.002Ω and ESR of L_3=0.012Ω
ESR of $C_1C_2C_4$ and C_5 is0.03Ω, ESR of C_3=0.015Ω
Total Loss in each reactive element is as follows:
$PL_{3AC}=4^2 \times 0.12 = 1.92W$
$PL_1=1.6^2 \times 0.002 = 0.00512W$
$PL_2=6.26^2 \times 0.002 = 0.0783W$
$PC_{3DC}=1^2 \times 0.015 = 0.015W$
While computing losses in capacitors on DC side, only ripple RMS current is considered for steady state condition.
$PC_2=1.6^2 \times 0.03 = 0.0768W$
$PC_1=6.26^2 \times 0.03 = 1.17W$
$PC_4=3^2 \times 0.03 = 0.27W$
$PC_5=4^2 \times 0.03 = 0.48W$

$P_{Reactive\ Elements}$=4.01W

D Efficiency

Total power loss in semiconductor devices:

$P=P_{switches}+P_{diodes}+P_{Reactive\ Elements}$

P=1.058+3.645+4.01=7.713W

Converter Efficiency is $\eta = \frac{100}{100+8.71} = 0.9098$

While Pin=$1.6 \times 8 + 6.26 \times 15 = 107W$

Pout=$19.4 \times 0.97 + 39.6 \times 1.98 = 97.226W$

DC and AC loads are resistive, and they are 20Ωeach.

$\eta = \frac{97.05}{107} = 0.91$

This experimentally observed efficiency.

VIII Conclusions

ASPWM based switching technique is adopted for the proposed hybrid output converter to enhance its ability to step up DC voltage and provide AC output at the second output port without use of inverter circuit. The performance of this converter is compared with conventional converter and inverter system, proposed hybrid converter is not only cost effective but also offers more benefits in usage. Less complexity is another feature of this converter as fewer switches are configured. It is suitable candidate for residential nano-grid rooftop application where ample and continuously solar energy is available. Conventional converter and inverter system leads to 82 to 85% efficiency while as hybrid output converter comes with 92%. It is tested for 100W in the laboratory. Other hybrid converters present in the literature are comparable in efficiency, but they offer less flexibility like one renewable input with high complexity in the circuit due to a greater number of power switches. Proposed output converter is solution to rooftop nano-grid application where simultaneous AC as well as DC power up to 1.5kW is obtained when 30V and 48 V DC sources are integrated with solar.

REFERENCES

[1] Anand,S. and Fernandes,B.G., “Optimal voltage level for DC microgrids,” IECON 2010-36th Annual Conference on IEEE Industrial Electronics Society, 2010.

[2] H.Behjati and A.Davoudi, "A new topology of multi-input multi-output Buck-Boost DC-DC Converter for microgrid applications",IEEE Transactions on Industry Applications,volume 49, 2013.

[3] A.Nahavandi, and M.T.Hagh,M.B.B.Sharifian,and S. Danyali, "A nonisolated multiinput multioutput DC–DC boost converter for electric vehicle applications",IEEE Transactions on Power Electronics,volume 30,year 2015.

[4] "E.Amiri,and Khorasani,R.and Adib,E. and A.Khoshkbar-Sadigh, “Multi-Input High Step-Up DC–DC Converter With Independent Control of Voltage and Power for Hybrid Renewable Energy Systems,” "IEEE Transactions on Industrial Electronics,volume 06,2011.

[5] P.Mohseni,and Hosseini,S.H. and Sabahi,M. and Jalilzadeh,T. and Maalandish,M, "A New High Step-Up Multi-Input Multi-Output DC–DC Converter", IEEE Transactions on Industrial Electronics,volume 66,2019.

[6] Kolahian,P.and Tarzamni,A. and Nikafrooz,A.and Hamzeh,M., "Multi-port DC--DC converter for bipolar medium voltage DC micro-grid applications", IET Power Electronics.volume 12,2019.

[7] Zeng,J.and Ning,X. and Du,K. and Taesic,Z. and Yang,V. and Winstead, "A four-port DC-DC converter for a standalone wind and solar energy system",IEEE Transactions on Industry Applications,volume 56,2019.

[8] Prabhakaran,P. and Agarwal,V, "Novel four-port DC--DC converter for interfacing solar PV,fuel cell hybrid sources with low-voltage bipolar DC microgrids",IEEE Journal of Emerging and Selected Topics in Power Electronics,volume 8,2018.

[9] Tian,Q. and Zhou,G. and Leng,M. and Xu,G. and Fan,X., "A nonisolated symmetric bipolar output four-port converter interfacing PV-battery system",IEEE Transactions on Power Electronics,volume 37,2010

[10] Vettuparambil,A. and Chatterjee,K. and Fernandes,B.G. "A multiport converter interfacing solar photovoltaic modules and energy storage with DC microgrid", IEEE Transactions on Industrial Electronics,volume 68,2020.

[11] Jiya,I.N. and Khang,H.V. and Kishor,N. and Ciric,M.R "Novel family of high-gain nonisolated multiport converters with bipolar symmetric outputs for DC microgrids", IEEE Transactions on Power Electronics,volume 37,2022.

[12] Madhana,R. and Geetha,M., " "Power enhancement methods of renewable energy resources using multiport DC-DC converter: A technical review", Sustainable Computing: Informatics and Systems,Elsevier,volume 37,2022.

[13] Bussa,V. and Ahmad,A. and Singh,R.K. and Mahanty,R. "Interleaved Hybrid Converter With Simultaneous DC and AC Outputs for DC Microgrid Applications", IEEE Transactions on Industry Applications,volume 54,2018.

[14] Ray,O. and Mishra,S., "Boost-Derived Hybrid Converter With Simultaneous DC and AC Outputs", IEEE Transactions on Industry Applications,volume 54,2014.

[15] Bagewadi,M.D. and Chobe,C. and Jagtap,P. and Siddique,M. and Dambhare,S. "Buck–boost derived interleaved hybrid converter for residential nanogrid applications", IET Power Electronics,volume 13,2020.
[16] Bhole,V. and Bagewadi,M.D. and Dambhare,S. Dual Input Dual Output Augmented SPWM based Hybrid Converter for DC Microgrid Application", IEEE Renewable Energy and Sustainable E-Mobility Conference (RESEM),2023.